

# Rapid prototyping of cyclic olefin copolymer based microfluidic system with CO<sub>2</sub> laser ablation

Jianchen Cai<sup>1</sup> · Jinyun Jiang<sup>1</sup> · Feng Gao<sup>2</sup> · Guangnan Jia<sup>2</sup> · Jian Zhuang<sup>2</sup> · Gang Tang<sup>2</sup> · Yiqiang Fan<sup>2</sup>

Received: 23 November 2016 / Accepted: 10 January 2017 / Published online: 19 January 2017  
© Springer-Verlag Berlin Heidelberg 2017

**Abstract** Cyclic olefin copolymer (COC) has high chemical resistance with low water absorption and good optical transparency in visual and near UV range, which is a promising material for the polymer-based microfluidic systems. A comprehensive method for the rapid prototyping of COC based microfluidic system using CO<sub>2</sub> laser ablation was proposed in this study. The COC substrate was fabricated by injection molding with a commercial injection molding machine, then CO<sub>2</sub> laser was used for direct laser ablation of microchannels on the surface of COC substrate, to seal the laser ablated microchannels, the thermal compression bonding method for COC-based substrates was also provided in this research. The profile of the microchannels was carefully studied with different laser ablation power and scan speed, microfluidic device fabricated using the proposed method were also presented in this research.

## 1 Introduction

Over the past decade, polymer materials have been widely used for the fabrication of microfluidic devices in biological (Macosko et al. 2015; Sackmann et al. 2014), medical (Chang et al. 2015; Warkiani et al. 2016) and chemical (Yücel et al. 2015; Zhou and Lin 2014) fields. Compare with glass, quartz or silicon with corresponding fabrication methods inherited from microelectronics, polymer

materials have the advantages of low-cost, wider variety of fabrication method (hot embossing, replica molding, laser ablation and etc.), disposable, and ease of surface modification. Some of the most frequently used polymer material in microfluidics includes polymethyl methacrylate (PMMA) (Battle et al. 2014), polycarbonate (PC) (Ogończyk et al. 2010), polystyrene (PS) (Hu et al. 2014) and polydimethylsiloxane (PDMS) (Lyu et al. 2014).

Cyclic olefin copolymer (COC) is another promising material for the fabrication of polymer-based microfluidic devices, compared with other polymer materials, COC has a better chemical resistance to hydrolysis, acetone and acids (Geschke et al. 2006) with a low water absorption (<0.01%) (Nunes et al. 2010), another crucial property of the COC is the high optical transparency in visual and near UV range (300–1200 nm).

Compare with the conventional photolithography (Chen et al. 2011), hot embossing (Wang et al. 2016), injection molding (Iwai et al. 2014) and replica molding (Iwai et al. 2014) methods for the fabrication of polymer-based microfluidic devices, CO<sub>2</sub> laser ablation is a direct, low-cost, and rapid alternative. During laser ablation, the focused laser beam scan along the predesigned route on the surface of the polymer substrate, since the process is purely thermal, the polymer material will melt down, decompose, and evaporate, finally formed the microchannel with a Gaussian profile. CO<sub>2</sub> laser has been previously used for the fabrication of PMMA (Chung and Tu 2013; Hong et al. 2010; Mohammed et al. 2015), PS (Li et al. 2012), glass (Niето et al. 2015), and paper-based (Spicar-Mihalic et al. 2013) microfluidic devices. Attempts have been made to provide numerical simulation of CO<sub>2</sub> laser ablation on COC/COP (Yi et al. 2008), or using micro-milling (Ogilvie et al. 2010) to fabricate COC-based microfluidic system. Rajeeb et al. used the hot embossing method for the fabrication of COC

✉ Yiqiang Fan  
fanyq@mail.buct.edu.cn

<sup>1</sup> College of Mechanical Engineering, Quzhou University, Zhejiang 324000, China

<sup>2</sup> College of Mechanical and Electrical Engineering, Beijing University of Chemical Technology, Beijing 100029, China

based microfluidic devices with silicon mold made with DRIE (deep reactive ion etching), Steigert et al. conducted the replica molding of COC-based microfluidic device using the SU-8 lithography with the epoxy mold. However, the fabrication process of COC-based microfluidic devices using CO<sub>2</sub> laser has not been intensively studied before.

In this study, for the first time, a comprehensive fabrication approach for the COC-based microfluidic devices using CO<sub>2</sub> laser ablation will be provided, which include the characterization of microchannel profile under different laser scan power and speed, and a thermal compression bonding method to seal the microchannels of COC substrates. For demonstration, microfluidic device fabricated using the proposed method is also presented in this study.

## 2 Materials and methods

### 2.1 Fabrication of blank COC substrate

COC pellet was obtained from TOPAS Advanced Polymers, Inc (KY, USA), with the model number 8007F-04. The preliminary drying process of the pellet was conducted in a vacuum oven (Thermo VT 6025, MA, USA) at 100 °C

for 2 h (at the atmospheric pressure) to remove the moisture which may cause the hydrolysis reaction in the followed injection molding process. During the injection molding process, the injection pressure was set at 75 MPa with a back pressure of 10 MPa and a screw speed of 150 rpm on an injection molding machine (HAITIAN MA 900 II, Zhejiang, China). The temperature settings of the heaters at different sections on barrel are shown in Fig. 1a. After cooling and demolding, the 1 mm-thick blank COC substrates with diameter of 50.8 mm by 76.2 mm were fabricated (shown in Fig. 1b).

### 2.2 Laser ablation process

The CO<sub>2</sub> laser ablation equipment (HTE-1206, Hantone CNC Equipment, Shandong, China) has the wavelength of 10.6 μm with the maximum power output of 80 W; the highest scanning speed of this laser ablation equipment is 500 mm/s, and the focal length of the laser head is 60 mm with the diameter of 60 μm for the focused spot. During the laser ablation process (shown in Fig. 2), the CO<sub>2</sub> laser beam was focused on the surface of COC substrate, causing the material to melt down, decompose and evaporate, the Gaussian heat distribution of the

**Fig. 1** **a** Heaters' temperature setup on barrel during the injection molding process of COC substrates using the injection molding machine. **b** Image of the inject molded COC substrates

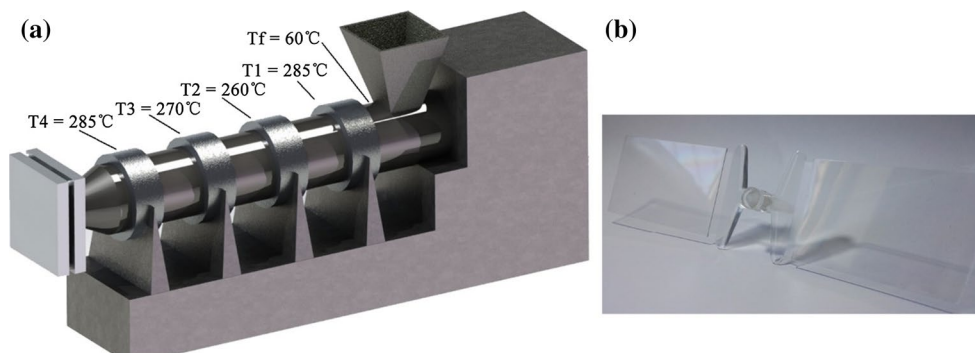


**Fig. 2** Schematic of the laser ablation system setup for the fabrication of microchannels on COC substrate

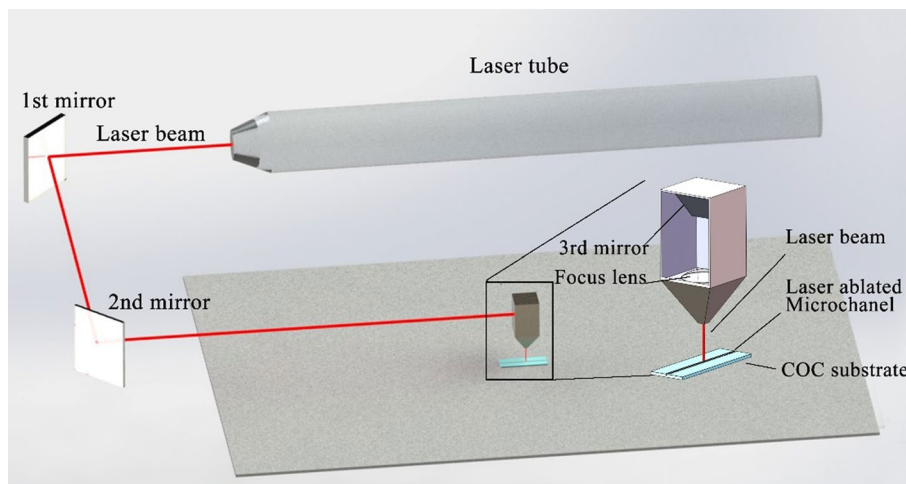


**Fig. 3** Schematic of the custom-made thermal compression bonding system setup, insert: the COC substrate and cover plate was sandwiched between two glass cover slips during the bonding process



laser beam result in a Gaussian-like profile of the ablated microchannel.

### 2.3 Thermal compression bonding

The laser ablated microchannels need to be sealed after the fabrication process for the followed biological or chemical applications, in this study, we proposed a simple and direct thermal compression bonding method to bond another layer of COC substrate to seal the fabrication microchannels. The thermal compression bonding method proposed in this study for the COC-based microfluidic devices is purely a physical processing approach, without any requirement for the chemical adhesives, which chemical adhesives may cause the contamination of the fluid sample inside the microchannel in the process of using.

A custom-made pneumatically driven thermal compression machine was used for the sealing of COC chipsets (shown in Fig. 3). During the thermal compression bonding process, the COC substrate with the laser ablated microchannel and a COC-based cover plate (both with the size of 25.4 mm by 76.2 mm, cleaned with ultra-sonic bath in DI water) were sandwiched between two glass cover slips with the same size for the protection of the contact surface during the thermal compression molding process (insert in Fig. 3). After that, the chipsets (two COC layers and two glass cover slips) were placed between the upper and lower heating plate, then start the heating and compression process simultaneously, the temperature at both heating plates (shown in Fig. 3) was set at 100 °C (with the ramp rate of 20 °C/min) with the compression pressure of 0.5 MPa (with the ramp rate of 0.1 MPa/min) on the chipsets. After temperature and compression reached the set values, the system was hold for 45 min to allow the long-chain polymer molecules on the contacted surface to entangle with

each other for a secured bonding. After the holding period, the electrical power on both heating plates was turned off for a natural cooling, the compression pressure could be removed with a rate of 0.5 MPa/min after the temperature on chipsets is lower than 45 °C. The secured bonding is achieved when the natural cooling of the chipsets reached the room temperature (24 °C). For piping, the silicone tubes (Silastic Laboratory Tubing 7-5224, Dow Corning Corporation) with outer diameter of 2 mm was used for the inlet and outlet ports.

The bonding temperature and pressure for the COC-based microfluidic devices are flexible due to size (width, depth and length) of microchannels fabricated on the surface of substrates. For a long and shallow microchannel, high temperature/pressure during the bonding process may cause the swell or even collapse of the microchannel; on the other hand, for a wide and deep microchannel, if the temperature or pressure setting is not high enough, the bonding between two polymer plates is not secure which may cause the fluid leak during the high-throughput test.

Figure 4a shows the laser ablated COC substrate (25.4 mm by 76.2 mm) and cover plate, Fig. 4b shows the T-shape droplet generator fabricated using the proposed fabrication method (photo taken by Canon 500D DSLR), the continues phase is mineral oil and the disperse phase is DI water dye with cresol red. For the microchannel fabrication, the power of the laser was set at 30 W with the scan speed of 250 mm/s to conduct the laser ablation process on the surface of COC substrate. During the thermal compression bonding process, the COC substrate with laser ablated microchannels was bonded with another COC cover plate (with laser ablated through holes for inlet and outlet ports) with the bonding temperature of 100 °C and bonding pressure of 0.5 MPa.

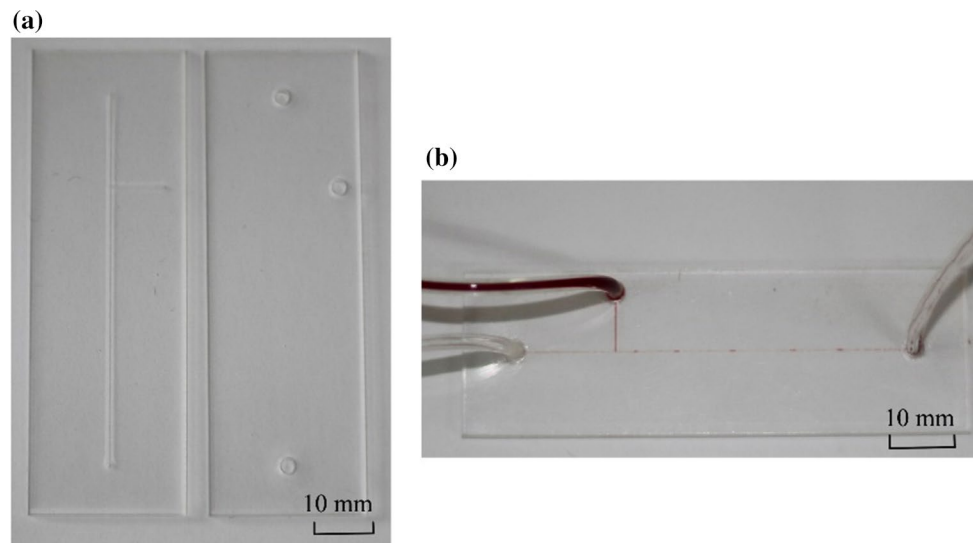


**Fig. 4** The CO<sub>2</sub> laser ablated droplet generator fabricated on the surface of COC substrate. **a** COC substrate with laser ablated microchannels and cover plate with laser ablated through holes. **b** The image of the fabricated COC-based T-shape droplet generator

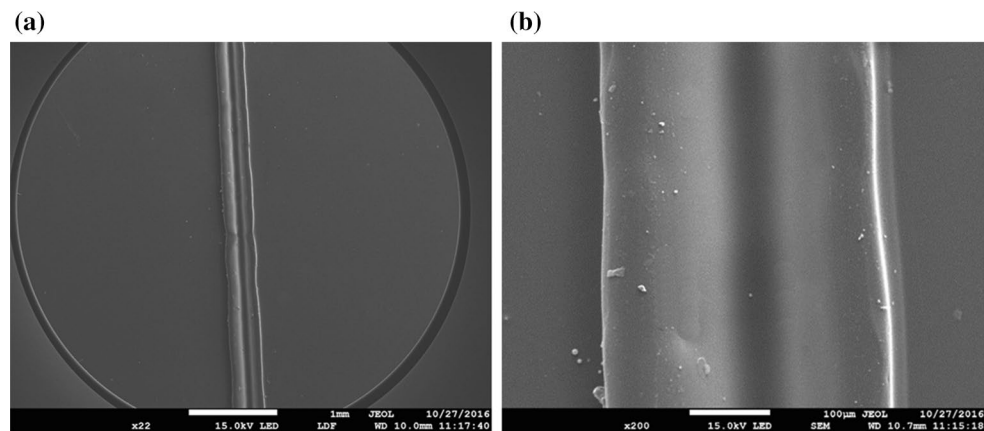


**Fig. 5** The SEM images for the laser ablated microchannels on COC substrate

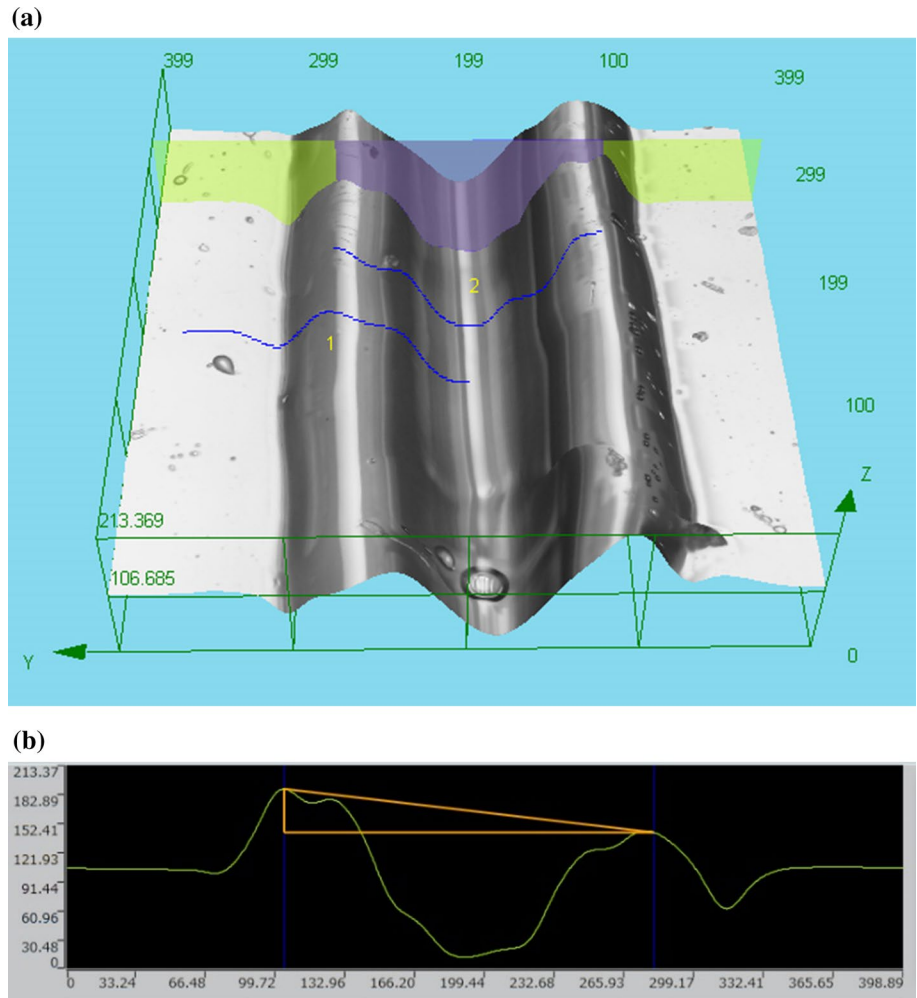
### 3 Result and discussion

For detailed characterization of the fabricated microchannels on COC substrates, the SEM images for the laser ablated microchannels (shown in Fig. 5) were taken by S-4700 field emission scanning electron microscope (Hitachi, Ltd., Japan). The microchannel shown in Fig. 4a, b was laser ablated on the surface of 1 mm-thick COC substrate with the power of 14 W and scan speed of 250 mm/s, with the channel width around 300 μm and depth around 200 μm. The bulges can be observed on both side of the microchannel, which caused by the ejection of molten polymer and re-solidification of the ejected polymer material on both side of the microchannel during the laser ablation and natural cooling process.

Figure 6a, b shows the cross section profile of the microchannel measured by OLS4100 3D laser confocal microscope (Olympus corporation, Japan), the microchannel shown in Fig. 6 was fabricated with the laser power of 12 W and scan speed of 300 mm/s, the width and depth and microchannel is 199 and 213 μm, respectively. The burgle height on each side of the microchannel is 58 and 43 μm, respectively. Furthermore, the width and depth of the microchannels fabricated under different laser power and scan speed were also measured using the 3D laser confocal microscope, which the result was plot in Fig. 7.

Figure 7 shows the width and depth of the microchannels fabricated under different laser power and scan speed, since the CO<sub>2</sub> laser ablation process is purely thermal, the laser power higher than 38 W or the scan speed

**Fig. 6** The profile of the microchannel measured by 3D laser confocal microscope. **a** The images of the laser ablated microchannel obtained from confocal microscope. **b** The cross-section profile of the laser ablate microchannel on COC



lower than 200 mm/s can easily cut through all the thickness of the 1 mm-thick COC substrate, and the microchannel can hardly be observed with laser power lower than 7 W, thus the range of the laser power used in this study is from 7 to 38 W with the scan speed ranges from 200 to 500 mm/s (500 mm/s is the maximum speed limitation of the instrument).

Due to the Gaussian-like cross section profile and the existence of bugles, the depth and width of the microchannel defined in this study is shown in the insert in Fig. 7. Figure 7 shows the width and depth of the microchannels under different laser power and scan speed, generally, the width and depth increase with higher laser power because more energy was transferred to polymer substrate for the formation of bigger molten pool under higher laser power, which result in a wider and deeper microchannel. We can also observe from Fig. 7 that, the width and depth of the microchannel will decrease with higher scan speed of the laser head, since higher scan speed lowered the average duration of stay for radiated

spot on the laser scan route, which less thermal energy was transferred during the ablation process and finally result in a smaller molten pool.

By choosing the laser ablation power and scan speed, microchannel with desired dimension can be achieved on the surface of COC substrate. The minimum width and depth can be achieved in this proposed method is around 223 and 132  $\mu\text{m}$ , respectively. The minimum feature can be achieved using the proposed method is limited from the  $\text{CO}_2$  laser equipment, this 3-axis CNC based laser ablation system has limited scan speed (maximum speed is 500 mm/s), and the focus point need to be manually adjusted using a gauge with the variation of the substrate thickness, thus the laser may not well focused on the surface of the polymer material during the ablation. Since the proposed fabrication method of the COC based microfluidic devices is a low-cost technique, the size of the microchannels can be achieved using the proposed method is suitable for the applications in biological field in most cases.

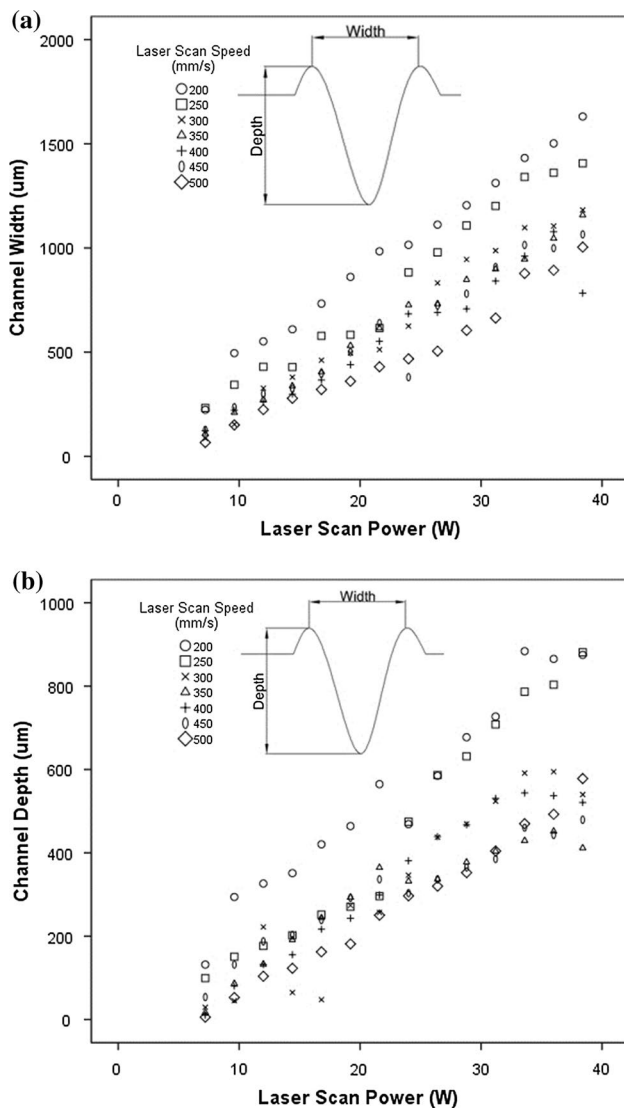


**Fig. 7** The depth and width of the microchannel under the different laser ablation power and scan speed. **a** The width of the microchannels under different laser ablation power and scan speed. **b** The depth of the microchannels fabricated using different laser power and scan speed

## 4 Conclusion

A comprehensive fabrication method for the low-cost and rapid prototyping of COC based microfluidic system using CO<sub>2</sub> laser ablation was proposed in this study. The blank substrates were obtained from injection molding, and the CO<sub>2</sub> laser equipment was used for the ablation of microchannels on the surface of COC substrates, and the depth and width of the microchannels were carefully studied under various laser power and scan speed. A thermal compression bonding approach was also provided for the simple and adhesive free sealing of the microchannels

fabricated on COC substrate. The microfluidic device for the demonstration of the proposed fabrication method was also provided in this study.

**Acknowledgements** This work was supported by Zhejiang Provincial Natural Science Foundation of China under Grant No. LQ16E030008, the Fundamental Research Funds for the Central Universities (ZY1613, buctrc201609), and the National Natural Science Foundation of China No. 51203010.

## References

- Battle KN, Jackson JM, Witek MA, Hupert ML, Hunsucker SA, Armistead PM, Soper SA (2014) Solid-phase extraction and purification of membrane proteins using a UV-modified PMMA microfluidic bioaffinity  $\mu$ SPE device. *Analyst* 139:1355–1363
- Chang KW, Li J, Yang CH, Shiesh SC, Lee GB (2015) An integrated microfluidic system for measurement of glycosylated hemoglobin Levels by using an aptamer–antibody assay on magnetic beads. *Biosens Bioelectron* 68:397–403
- Chen W, Lam RH, Fu J (2011) Photolithographic surface micromachining of polydimethylsiloxane (PDMS). *Lab Chip* 12:391–395
- Chung CK, Tu KZ (2013) Application of metal film protection to microfluidic chip fabrication using CO<sub>2</sub> laser ablation. *Microsyst Technol* 20:1987–1992. doi:10.1007/s00542-013-2041-3
- Geschke O, Perozziello G, Bundgaard F (2006) Rapid prototyping tools and methods for all-Topas<sup>®</sup> cyclic olefin copolymer fluidic microsystems. *Proc Inst Mech Eng Part C: J Mech Eng Sci* 220:1625–1632. doi:10.1243/09544062jmes295
- Hong T-F, Ju W-J, Wu M-C, Tai C-H, Tsai C-H, Fu L-M (2010) Rapid prototyping of PMMA microfluidic chips utilizing a CO<sub>2</sub> laser. *Microfluid Nanofluid* 9:1125–1133. doi:10.1007/s10404-010-0633-0
- Hu X, Lin X, He Q, Chen H (2014) Electrochemical detection of droplet contents in polystyrene microfluidic chip with integrated micro film electrodes. *J Electroanal Chem* 726:7–14
- Iwai K, Shih KC, Lin X, Brubaker TA, Sochol RD, Lin L (2014) Finger-powered microfluidic systems using multilayer soft lithography and injection molding processes. *Lab Chip* 14:3790–3799
- Li H, Fan Y, Kodzius R, Foulds IG (2012) Fabrication of polystyrene microfluidic devices using a pulsed CO<sub>2</sub> laser system. *Microsyst Technol* 18:373–379
- Lyu SR, Chen WJ, Hsieh WH (2014) Measuring transport properties of cell membranes by a PDMS microfluidic device with controllability over changing rate of extracellular solution. *Sens Actuators B Chem* 197:28–34
- Macosko E et al (2015) Highly parallel genome-wide expression profiling of individual cells using nanoliter droplets. *Cell* 161:1202–1214
- Mohammed MI et al (2015) Improved manufacturing quality and bonding of laser machined microfluidic systems. *Proc Technol* 20:219–224
- Nieto D, Couceiro R, Aymerich M, Lopez-Lopez R, Abal M, Flores-Arias MT (2015) A laser-based technology for fabricating a soda-lime glass based microfluidic device for circulating tumour cell capture. *Colloids Surf B Biointerfaces* 134:363–369. doi:10.1016/j.colsurfb.2015.07.007
- Nunes PS, Ohlsson PD, Ordeig O, Kutter JP (2010) Cyclic olefin polymers: emerging materials for lab-on-a-chip applications. *Microfluid Nanofluid* 9:145–161. doi:10.1007/s10404-010-0605-4
- Ogilvie IRG, Sieben VJ, Floquet CFA, Zmijan R, Mowlem MC, Morgan H (2010) Reduction of surface roughness for optical quality

- microfluidic devices in PMMA and COC. *J Micromech Microeng* 20:065016. doi:[10.1088/0960-1317/20/6/065016](https://doi.org/10.1088/0960-1317/20/6/065016)
- Ogończyk D, Węgrzyn J, Jankowski P, Dabrowski B, Garstecki P (2010) Bonding of microfluidic devices fabricated in polycarbonate. *Lab Chip* 10:1324–1327
- Sackmann EK, Fulton AL, Beebe DJ (2014) The present and future role of microfluidics in biomedical research. *Nature* 507:181–189
- Spicar-Mihalic P, Toley B, Houghtaling J, Liang T, Yager P, Fu E (2013) CO<sub>2</sub> laser cutting and ablative etching for the fabrication of paper-based devices. *J Micromech Microeng* 23:067003. doi:[10.1088/0960-1317/23/6/067003](https://doi.org/10.1088/0960-1317/23/6/067003)
- Wang X, Liedert C, Liedert R, Papautsky I (2016) A disposable, roll-to-roll hot-embossed inertial microfluidic device for size-based sorting of microbeads and cells. *Lab Chip* 16:1821–1830
- Warkiani ME, Khoo BL, Wu L, Tay AKP, Bhagat AAS, Han J, Lim CT (2016) Ultra-fast, label-free isolation of circulating tumor cells from blood using spiral microfluidics. *Nat Protoc* 11:134–148
- Yi L, Xiaodong W, Fan Y (2008) Microfluidic chip made of COP (cyclo-olefin polymer) and comparison to PMMA (polymethylmethacrylate) microfluidic chip. *J Mater Process Technol* 208:63–69. doi:[10.1016/j.jmatprotec.2007.12.146](https://doi.org/10.1016/j.jmatprotec.2007.12.146)
- Yücel M, Beaton AD, Dengler M, Mowlem MC, Sohl F, Sommer S (2015) Nitrate and nitrite variability at the seafloor of an oxygen minimum zone revealed by a novel microfluidic in-situ chemical sensor. *Plos One* 10:e0132785
- Zhou Y, Lin Q (2014) Microfluidic flow-free generation of chemical concentration gradients. *Sens Actuators B Chem* 190:334–341